Modulating the ER stress response attenuates neurodegeneration in a *C. elegans* model of spinal muscular atrophy

James J. Doyle[1, 2], Celine Vrancx[3], Claudia Maios[3], Audrey Labarre[3], Shunmoogum A Patten[4], J. Alex Parker[3]

1 Division of Experimental Medicine, McGill University, Montreal, Quebec, Canada

2 Metabolic Disorders and Complications, RI-MUHC, Montreal, McGill, Canada

3 CRCHUM and Department of Neuroscience, University of Montreal, Montreal, Quebec, Canada

4 INRS-Institut Armand-Frappier, Laval, Quebec, Canada

*Corresponding author at:

CRCHUM, Tour Viger, 900, rue Saint-Denis, R09.440

Montréal, Québec, Canada, H2X 0A9 Tel.: +1 514-890-8000 ext. 28826. Fax: +1 514 412-7602

E-mail address: ja.parker@umontreal.ca (J.A. Parker);

Significance

Spinal muscular atrophy (SMA) is a devastating neuromuscular condition resulting from decreased levels of the SMN1 protein. Although a large proportion of research into SMA has focused on the neuronal role of the protein, SMN1 is expressed in many different tissue types and its role in them has often been overlooked. In this study, we demonstrate that muscle dysfunction precedes the onset of neurodegeneration in a simple genetic model of SMA. Additionally, we show that targeting endoplasmic reticulum (ER) stress in non-neuronal cells suppresses many of the phenotypes associated with SMA in our model, and this protective effect is enhanced when we supplement neuromuscular junction-targeting therapeutics. Together, our findings open up new therapeutic targets for SMA.

Abstract

Spinal muscular atrophy is (SMA) is a devastating, autosomal recessive neuromuscular disease resulting in muscle atrophy, neurodegeneration, and is the leading genetic cause of infant death. SMA arises when there are homozygous deletion mutations in the human *SMN1* gene, leading to a decrease in corresponding SMN1 protein. Although SMN1 is expressed across multiple tissue types, much of the previous research into SMA focused on the neuronal aspect of the disease, overlooking many of the potential non-neuronal aspects of the disease. Therefore, we sought to address this gap in knowledge by modeling SMA in the nematode *Caenorhabditis elegans*. We used a previously uncharacterized allele which resulted in the onset of mild SMA-like phenotypes allowing us to monitor the onset of phenotypes at different stages. We observed that these mutant animals recapitulated many key features of the human disease, and most importantly, we observed that muscle dysfunction precedes neurodegeneration. Furthermore, we tested the therapeutic efficacy of targeting endoplasmic reticulum (ER) stress in non-neuronal cells and found it to be more effective than targeting ER stress in neuronal cells. We also found that the most potent therapeutic potential came from a combination of ER- and neuromuscular junction (NMJ)-targeting drugs. Together, our results suggest an important non-neuronal component of SMA pathology and highlight new considerations for therapeutic intervention.

Introduction

Spinal muscular atrophy (SMA) is an autosomal recessive neuromuscular disorder of early childhood. The incidence of SMA is approximately 1 in 10,000 live births, and it is reported to be the leading genetic cause of infant death (1, 2). SMA is characterized by the progressive loss of motor neurons in the anterior horn of the spinal cord (3). This degeneration leads to muscle weakness and atrophy, primarily affecting proximal muscles and lung muscles, resulting in limb paralysis, respiratory failure, and death. SMA can manifest itself in several degrees of severity but all have in common progressive muscle atrophy and mobility impairment.

In humans, there are two copies of the *Survival Motor Neuron* gene, *SMN1* and *SMN2*. The *SMN2* gene is almost identical to the *SMN1* gene, with the difference being that it holds a C-to-T nucleotide exchange at position 6 of exon 7, responsible for the skipping of exon 7 during splicing (4). This alternative splicing causes 90% of transcripts to result in a truncated protein, SMNΔ7, which degrades rapidly. The other 10% undergo correct splicing, thus producing a small amount of SMN protein. In healthy individuals, the *SMN1* gene can compensate for overall SMN protein production, however, in more than 90% of SMA cases, there is a homozygous deletion or mutation in the *SMN1* (5, 6) gene resulting in an inability of *SMN1* to counterbalance SMN protein levels. Under normal circumstances, SMN1 is involved in many aspects of RNA processing in cells, notably in the splicing of pre-mRNA to mRNA (7). It is also required for proper neuronal outgrowth to form axons and dendrites.

Since *SMN1* and *SMN2* are evolutionarily conserved, we used the nematode *Caenorhabditis elegans* to develop a new, biologically relevant animal model to study SMA pathology (8). Although nematodes and humans are evolutionarily distant, genetically they share a high degree of conservation and *C. elegans* has been widely used to model many aspects of neurodegeneration (9). Both human *SMN1* and *SMN2* genes have a single ortholog in nematodes, named *smn-1* (8). Previous studies into *C. elegans smn-1* have primarily utilized the *ok355* deletion mutant which, as in humans, results in lethality (10-16). Although it recapitulates the aspects of the human disease, it is impractical to study finer aspects of the disease such as phenotype and symptom onset. For this, we sought to study *smn-1* mutations using a mild mutant allele. Using the *gk118916* allele, which has a C-to-T nucleotide exchange in the 4th exon of *smn-1*, we show that animals with this mild mutation still exhibits key features of the human disease, including reduced lifespan, progressive, age-dependent paralysis, and neurodegeneration, but do not show a strong larval-lethal phenotype. Furthermore, a key feature apparent in SMA is the presence of ER stress (17) which arises from the abnormal splicing of ER chaperones. This feature is also conserved in our nematode model and is a potential therapeutic target.

Although much of the previous research into SMA has focused on the role of SMN1 in neurons and on the neuronal component of SMA's pathology, SMN1 is expressed in many tissues and cell types. Therefore, it may be informative to investigate SMN1 and SMA pathology beyond their neuronal components (18). In this study, we used the *smn-1(gk118916)* allele (hereby noted as *smn-1(gk)*) to generate a moderate SMA model. The mild model has many advantages over the severe lethal alleles, notably that it is possible to study the temporal onset of several

phenotypes in the model. We discovered that, surprisingly, muscle degeneration precedes neurodegeneration, and that genetically inhibiting ER stress in non-neuronal cells alone suppressed degenerative phenotypes. We further show that a combination of small molecules targeting both ER stress and neuromuscular junctions is more effective than the individual treatments. Together, our results introduce a new genetically relevant model to study SMA which can be used for SMA drug discovery and development.

Results

An *smn-1* point mutation leads to motor defects and neurodegeneration in *C. elegans*

The C-to-T nucleotide change in the chosen *smn-1* allele, *gk118916*, results in an E167K missense mutation at the protein level and was generated by the Million Mutation Project (MMP) (19). Although not a splice-site mutation as found in humans, the amino acid change from a negatively-charged glutamine (E) residue to a positively-charged lysine (K) is predicted to impair the SMN-1 protein's structure. *smn-1(gk)* mutant animals do not display any gross developmental problems and appear superficially normal, but upon closer inspection of adult worms we observed a reduction in lifespan (Fig. 1A). The normal development into adulthood helps remove the constraints on studying SMA in *C. elegans* as this viable allele allows for a wider range of analyses. We also observed motility defects in these animals leading age-dependent paralysis a few days after the worms entered adulthood (Fig. 1B).

Since SMA is caused by mutations resulting in decreased SMN protein levels, we hypothesized that the paralysis phenotype observed in *smn-1(gk)* mutants was due to an insufficient level of wild-type SMN-1 protein. We investigated this possibility by crossing the *smn-1(gk)* strain to wild-type N2 animals to create *smn-1(gk)*/+ animals, and we observed that the level of paralysis for these heterozygotes was less than *smn-1(gk)/smn-1(gk)* mutants, but greater than wild type +/+ N2 worms (Fig. 1C). Lacking a functional antibody targeting the endogenous SMN-1 protein, we looked at gene expression levels of *smn-1* mRNA and saw a slight, non-significant increase in *smn-1* transcript levels in *smn-1(gk)* animals compared to N2 controls (Fig. 1D). Although not significant, this increase in mRNA levels could be explained by a feedback mechanism seeking to compensate for a loss of SMN-1 protein's normal function. Together, these data suggest that *smn-1(gk)* acts in a semi-dominant manner and the paralysis phenotype may correspond to a partial loss of SMN-1 protein function, as opposed to a decrease in the total amount of SMN-1 protein.

Motility problems can be a sign of neuronal dysfunction and/or neurodegeneration, as we have previously observed in our worm models of amyotrophic lateral sclerosis (ALS) (20). To investigate the possibility of motor neuron degeneration we crossed the *smn-1(gk)* mutants with transgenic reporter strains expressing fluorescent proteins in GABAergic (21) or cholinergic motor neurons. Degeneration of motor neurons was assessed by scoring for the presence of breaks, or gaps along the ventral nerve cord (Fig. 1E). Compared to wild type controls, at day 9 of adulthood we observed a significant increase in degeneration of GABAergic motor neurons, but no significant difference was noted for cholinergic motor neurons (Fig. 1F).

Since human *SMN1* mutations that lead to SMA are a complete loss-of-function (LOF), we sought to better understand the nature of the mutations in the *smn-1(gk)* nematodes. We therefore used RNA interference (RNAi) to further reduce the amount of *smn-1* available and observed a significant increase in paralysis in *smn-1(gk)-smn-1(RNAi)* animals, but did not see a further enhancement of neurodegeneration (Fig. 1G-H). These data suggest the *smn-1(gk)* is a hypomorphic allele resulting in a partial LOF.

We sought to further identify phenotypes characteristic of these *smn-1(gk)* nematodes and so we assessed their ability to swim. When nematodes are placed in a liquid medium such as M9, worms change their characteristic crawling movement for a thrashing swim-like motion which can be analyzed over a period of time. We assayed for swimming at both day 1 and day 5 of adulthood and observed that *smn-1* mutants did not display any difficulty swimming at day 1 (data not shown) but there was a clear impairment of swimming at day 5 (Fig. 1I) compared to N2 control animals. The onset of impaired swimming defects correlated with the onset of the paralysis phenotypes for *smn-1(gk)* worms grown on solid media. Since there was no observable neurodegeneration at earlier stages (days 3 and 5, Fig. 1J), we sought to identify the causes of the swimming and paralysis phenotypes. We have shown in previous work that neurotransmission is affected in *C. elegans* models of ALS, and since ALS and SMA are very similar clinically (22) we tested synaptic function in *smn-1(gk)* animals. Upon treatment with aldicarb, an acetylcholinesterase inhibitor (23), *smn-1* mutant worms displayed a hypersensitivity and paralyzed sooner than control animals, but not to the extent of *unc-47(e307)* positive control animals (Fig. 1K). This suggested that our *smn-1(gk)* animals may have neuromuscular junction (NMJ) defects.

A common criticism of strains generated by the MMP is that they contain on average ~400 mutations. As a result, even after 6 rounds of outcrossing, there is a risk that any phenotype potentially linked to a mutation of interest may be due to another mutation that remained in the strain background. Therefore, we used CRISPR/Cas9 (24-27) to introduce the *gk118916* allele into wild-type N2 animals to see if they would exhibit similar phenotypes. As observed, our CRISPR mutants, *smn-1(syb1923)*, exhibited slightly higher levels of paralysis compared to *smn-1(gk)* animals but had a nearly identical swimming defect (Fig. 1L-M). These CRISPR animals also displayed significant levels of neurodegeneration in their GABAergic neurons (Fig. 1N). Therefore, we can conclude that phenotypes observed in *smn-1(gk)* animals can be attributed to the *gk118916* allele and not to a background mutation still present in the strain. Together, these data show that *smn-1(gk)* may be a suitable and relevant model to study SMA as it recapitulates many key features of the disease. Lastly, since we observed that motility defects can be detected in the absence of neurodegeneration, there may be additional factors contributing to impaired movement of *smn-1* mutants.

smn-1(gk) mutations lead to loss of muscle cell integrity

It is widely accepted that SMA is a neuromuscular disorder, however we wanted to investigate if the *smn-1(gk)* mutants had any non-neuronal consequences. We tested *smn-1(gk)* animals for their sensitivity to levamisole, a nicotinic acetylcholine receptor agonist (nAChR) (28). Since nAChR are solely expressed in body-wall muscle cells, this assay is used to identify potential defects in the worms' muscle cells. We observed that day 1 adult *smn-1(gk)* animals were

hypersensitive to levamisole, suggesting the presence of very early muscle defects (Fig. 2A). We therefore performed the non-neuronal RNAi knock-down of *smn-1* in wild-type N2 animals and in a transgenic strain sensitive to RNAi specifically in body-wall muscle cells (Fig. 2B-C). It was evident that RNAi-mediated depletion of *smn-1* was sufficient to induce paralysis phenotypes in these two strains, but the depletion of *smn-1* only in intestinal cells had no effect on animal health. (Fig. 2D). These data suggest there may be a contribution of SMN-1 in muscle cells to worm health and viability.

We then sought to investigate if there was any evidence of muscle morphological defects in *smn-1(gk)* animals. We used a recombinant myosin protein tagged with GFP, MYO-3::GFP (29), to visualize muscle integrity. Under normal circumstances, the MYO-3::GFP signal can be observed as regular, linear filaments within the body-wall muscles, as would be expected from myosin filaments (29, 30). However, we observed that with age we saw the appearance of irregular shapes, or disorganized GFP, suggesting a loss of myosin structural integrity, and a likely a loss of general muscle structure. We characterized the extent of this disorganization as "Low", "Medium", or "High" (Fig. 2E), which allowed us to quantify this morphological defect. As early as day 3 of adulthood, we observed a significant increase of *smn-1(gk)* animals with high levels of disorganization compared to WT animals (Fig. 2F), and this effect was worsened in day 5 animals (Fig. 2G). This phenotype was also present in *smn-1(syb1923)* CRISPR mutants at day 5 (Fig. 2H). Similarly, we quantified levels of mitochondrial fragmentation in body-wall muscle cells using a TOM20::mRFP reporter as a complementary assay of muscle health. We characterized mitochondrial organization as "Linear", "Intermediate", or "Fragmented" (Fig. 2I), as previously described (31, 32). We observed that as early as day 1, we see a significant increase in levels of

"Fragmented" mitochondria (Fig. 2J), with this effect being significantly aggravated by day 5 (Fig. 2K). In light of our observations about the lack of neurodegeneration at days 3 to 5 in adult *smn-1* mutants (Fig. 1I), our data suggests that in the absence of wild type levels of SMN-1 protein, muscle cell defects occur prior to motor neuron degeneration, a phenomenon that may have implications in the design of therapeutic approaches for SMA.

Small molecule regulators of ER stress rescues SMA-like phenotypes in *C. elegans*

Previously, our group has studied the role of endoplasmic reticulum (ER) stress in ALS models and we identified compounds able to correct motor neuron phenotypes in *C. elegans* and zebrafish (33). Since ALS and SMA share many clinical and molecular features we tested whether two ER stress-targeting compounds, guanabenz or salubrinal, had protective effects in our *smn-1(gk)* model. We observed that treatment with either compound rescued paralysis and neurodegeneration phenotypes in mutant *smn-1* animals (Fig. 3A-B). Furthermore, when we treated worms with the compounds from the L4 larval stage until day 5 of adulthood and we observed a marked reduction in muscle defects apparent in the mutant animals (Fig. 3C). The protective effects of both compounds were maintained in *smn-1(syb1923)* mutants against their paralysis, neurodegeneration, and muscle defects (Fig. 3D-F).

Targeting ER stress in non-neuornal cells alleviates motor neuron degeneration

Since muscle defects appear earlier than neuronal problems in *smn-1* mutants, we next wanted to investigate if targeting ER stress in non-neuronal cells would have a stronger beneficial effect than in neuronal cells. In *C. elegans*, neuronal cells are naturally resistant to RNAi knock-

down and must be genetically modified to be sensitive to RNAi in neurons. Therefore, when non-transgenic animals are treated with RNAi, the knock-down effect is mainly experienced in non-neuronal cells. We used RNAi against *ire-1*, *atf-6*, and *pek-1*, three upstream effectors of ER stress and nematode orthologues of human IRE1, ATF6, and PERK (33, 34), respectively, and empty vector (EV) control. When *smn-1* mutants were treated with non-neuronal ER RNAi from the L4 stage, we observed a significant decrease in progressive paralysis, neurodegeneration in day 9 animals, and muscle defects in day 5 adult animals (Fig. 3G-I). These results were unexpected and suggest that that genetically blocking ER stress in non-neuronal cells can reduce the degeneration of motor neurons.

To see if the age-related phenotypes due to *smn-1(gk)* mutations could be reversed at a later stage, we treated mutant animals with non-neuronal RNAi against *ire-1*, *atf-6*, and *pek-1* commencing at day 5 of adulthood. We saw a significant decrease in paralysis levels in these animals as compared to the EV controls (Fig. 3J), which also suggests the effects of *smn-1(gk)* are not just developmental in origin. In contrast, when we treated worms with neuronal-specific RNAi, we saw no effect of the gene knockdown on paralysis, and very little effect on neurodegeneration (Fig. 3K-L). Together, these data point to an important role for ER stress in non-neuronal cells in animals with *smn-1* mutations and, from a therapeutic standpoint, targeting ER stress in non-neuronal cells appears may be effective and can complement neuronal-focused therapies.

Enhanced protection from targeting the NMJ and ER stress response

Given the similarities between ALS and SMA, we decided to examine whether clinically-tested drugs for ALS could would show protective effects in a genetic model for SMA. We selected riluzole, a widely used ALS therapeutic, and pimozide, a neuroleptic recently identified by our group and validated in a small-scale clinical trial for ALS (35). We tested these two compounds for their ability to restore swimming behavior in *smn-1* mutants at day 5 of adulthood, and found that pimozide, but not riluzole, was able to significantly improve this behavior (Fig. 4A). However, both these drugs were able to suppress paralysis and neurodegeneration for *smn-1* mutants grown on solid media (Fig. 4B-C). We next examined muscle cell defects, and we observed that of the two compounds, only pimozide suppressed muscle phenotypes in *smn-1* mutants (Fig. 4D), and this is consistent with the hypothesis that pimozide acts by stabilizing the NMJ.

Since we had identified compounds that could independently restore paralysis, neurodegeneration, and muscle defects in *smn-1(gk)* animals, we decided to test if they could act synergistically to better improve the animals' health. We tested each compound at half the dose previously tested, or 20 µM for pimozide and 25 µM for salubrinal. We observed that this combination suppressed paralysis in *smn-1(gk)* animals, and rescued muscle morphology defects in *smn-1* mutants at day 5 of adulthood (Fig. 4E-F). However, these compounds, tested individually and given as of day 5 of adulthood, had little effect on suppressing paralysis in *smn-1* mutants (Fig. 4G); when both drugs were combined, though, and treated as of day 5 of adulthood there was a reduction in paralysis (Fig. 4H). Together our results suggest that early treatment by combining salubrinal and pimozide to simultaneously block ER stress and stabilize

the NMJ is effective in rescuing *smn-1* mutant phenotypes. Therefore, this combination, if validated, could open up new therapeutic treatments for SMA patients. Furthermore, our results suggest that the timing window for delivery of this combination is limited and should be taken into consideration.

Discussion

In this study, we show that a point mutation in *C. elegans smn-1* results in phenotypes of moderate severity, and allowed us to study the molecular signature of *smn-1* shedding new light on SMA pathology. We show that the onset of muscular dysfunction precedes neurodegeneration and that targeting therapies to muscle cells is more effective than neuronal delivery. The information gained from this model could not have been obtained from the extensively studied *C. elegans smn-1(ok355)* deletion mutant as this results in a severe lethal phenotype, which masks the appearance of certain phenotypes or makes them difficult or impossible to study. For example, our model here is the first nematode *smn-1* model with a genetic mutation to show neurodegeneration, a phenotype which could not be seen in the *ok355* mutant (11, 36, 37). By using an allele that generates mild SMA-like characteristics, much like the previously-studied *smn-1(cb131)* (38), we were able to gradually monitor the onset of specific aspects of SMA pathology. However, despite the differences between our model and the reference *ok355* allele, many of the key phenotypes are conserved including decreased lifespan, motility defects, and changes in aldicarb sensitivity (10, 11).

One of the key pieces of information gained in this study was that we observe the onset of muscle dysfunction in advance of neurodegeneration, and that modulating ER stress in non-neuronal cells is sufficient to rescue neurodegeneration. We hypothesize that muscle dysfunction may contribute neurodegeneration in SMA, where after the onset of muscular dysfunction, it is possible that neurons could lose their NMJ connections and in turn degenerate. If verified in other systems, this information could change how we approach gene therapy for SMA. Current approaches focus on driving full-length SMA into neuronal cells thereby re-expressing the full-length functional protein in these cells. To date, this approach has been very successful, however, the efficiency fails if it is delivered to SMA patients after they reached 6 months of age, and we do not yet know the long-term effects of this approach. If our hypothesis is confirmed, the current success of neuronal gene therapy approaches could be attributed to SMN1-expressing neurons supporting muscles and slowing their degeneration. Since we do not yet know the long-term clinical outcomes, we cannot determine if the neuronal SMA gene therapy will continually support muscles, or if there will come a point where the neuronal support will no longer be sufficient and muscles will continue to degenerate. Furthermore, if our hypothesis is correct, it could help explain why the current approach fails in patients after 6 months of age; it is possible muscle degeneration reaches a certain threshold beyond which the SMN1-expressing neuronal support fails to have any effect. Although it may take years before the necessary clinical information becomes known, our results suggest that muscle degeneration in SMA may be an important driver of neurodegeneration and this information should be considered for future gene therapy efforts.

Although a combination of neuronal- and muscle-driven gene therapy for SMA will very likely benefit a large number of patients, it is likely that not all affected individuals will respond equally to this therapeutic approach. Therefore, developing other therapeutic approaches using small molecules is also of utmost importance. In this study, we show that a combination of two pharmacological compounds, pimozide and salubrinal, was more beneficial than each one individually. To target the ER stress in SMA, we utilized salubrinal, a specific inhibitor of eIF2a (39). This showed promise in restoring paralysis, neurodegeneration, and muscle defects in our *smn-1(gk)* model. The second compound, pimozide, is a neuroleptic which has been used as an anti-psychotic agent for many years, and was recently identified by our group in a chemical-genetic screen for TDP-43 toxicity in ALS and was validated in a small Phase 2a clinical trial. In ALS, pimozide was hypothesized to stabilize the NMJ in ALS and therefore delayed the onset of neurodegeneration. Given the large clinical overlap between SMA and ALS, we decided to test pimozide in our SMA model and it was also able to rescue key phenotypes. Since pimozide was able to prevent muscle dysfunction, we believe this supports the hypothesis of pimozide stabilizing the NMJ. Interestingly, we also tested riluzole, an approved therapeutic for ALS, and although it was able to restore motility and neurodegeneration in *smn-1* mutants, it showed no effect on muscle health. Previously, riluzole was shown to activate calcium-activated potassium channels which are mainly expressed in neurons in *C. elegans* (13). The differences between pimozide's and riluzole's effects in our *smn-1* model suggests a different mechanism of action and broadens the potential for pimozide to treat a range of neuromuscular disorders. The therapeutic application of pimozide resembles the stabilizing action that neuron-driven SMN1 expression has on muscles, and therefore could explain its beneficial effects. In combination,

however, these drugs appear to act synergistically to target both ER stress in non-neuronal cells and to stabilize the NMJ further supporting muscle integrity.

Altogether, our data show an essential non-neuronal contribution of *smn-1* to neuronal survival. We also show that a combination of therapies modulating ER stress and NMJ stabilization result in dramatically improved muscle health. We suspect the ER-modulating drugs are acting on muscle cells, the most likely cell type to respond to this treatment in the face of *smn-1* mutations. Although we acknowledge that these results need to be validated in other model systems, we propose that the information gained here could be applied to the development of future therapeutic efforts for SMA. Also, despite recent advances in gene therapy technology, its future remains uncertain and its success cannot be guaranteed in all patients. Therefore, it remains important to develop alternative, small molecule therapeutics which can be orally administered to patients while they await a genetic diagnosis, or to be used in conjunction with current gene therapy approaches. This is more advantageous if these molecules can be repurposed from other diseases thereby eliminating the need for the time-intensive regulatory process needed to take new molecules to market.

Materials and Methods

C. elegans strains

All nematodes were cultured and handled as per standard methods. The following strains were used (STRAIN NAME/*genotype*): N2, *smn-1(gk118916)*, LX929/*vsIs48[unc-17::GFP]*, *ufIs34[Punc-47::mCherry]*, DM8005/*raIs5[myo-3p::GFP::myo-3 + rol-6(su1006)]*, *smn-1(gk118916); raIs5 [myo-3p::GFP::myo-3 + rol-6(su1006)]*, TU3311/*uIs60 [unc-119p::YFP + unc-119p::sid-1]*, *smn-1(gk118916); uIs60[unc-119p::YFP + unc-119p::sid-1]*, VP303/*rde-1(ne219)*; *kbIs7 [nhx-2p::rde-1 + rol-6(su1006)]*, NR350/*rde-1(ne219)*; *kzIs20 [hlh-1p::rde-1 + sur-5p::NLS::GFP]*, PS6192/*syIs243 [myo-3p::TOM20::mRFP + unc-119(+) + pBS Sk+].* Mutant *smn*-1 worms were outcrossed 6 times to wild-type N2 worms before use. Genotyping of the *smn-1(gk)* mutation was performed by high-resolution melting (HRM) using HRM MeltDoctor reagents (Applied Biosystems) and analyzed on HRM software (Applied Biosystems). Verification by Sanger sequencing was performed by Genome Quebec (McGill University). The *C. elegans smn-1 gk118916* allele was recapitulated in wild-type N2 animals by SunyBiotech using CRISPR-Cas9; this strain was called *smn-1(syb1923)*. All experiments were carried out at 20°C and were repeated a minimum of three times.

Paralysis assays

For all strains, 25-30 L4 animals were picked to NGM plates and scored daily starting the following day at day 1 of adulthood. Worms were counted as paralyzed if they failed to move their body upon prodding with a platinum wire. Worms were considered dead if they failed to move their head when prodded and showed no pharyngeal pumping; dead worms were censored from statistical analyses. For paralysis assays with chemical compounds, worms were grown on standard NGM plates and transferred onto NGM + drug or NGM + DMSO control plates at the L4 stage. Worms were scored as described above. Together, a minimum of 250 animals were scored per genotype and condition.

Lifespan assays

For all strains, 25-30 L4 animals were picked to NGM plates and scored every second day from day 1 of adulthood until death. Worms were considered dead if they failed to respond to mechanical or heat stimulus and showed no pharyngeal pumping. A minimum of 250 animals were scored per genotype.

Aldicarb and levamisole assays

Worms were grown on NGM plates and transferred to NGM plates spiked with 1 mM aldicarb, or 0.5 mM levamisole, at day 1 of adulthood. Paralysis was scored every 30 minutes for 2 hours for aldicarb assays, or every 15 minutes for 1 hour for levamisole assays. Animals were considered paralyzed if they failed to respond to gentle prodding with a platinum pick. A minimum of 250 animals were scored per genotype.

Liquid culture motility assays

Synchronized, age-matched worms were rapidly picked into 96-well plates containing M9 buffer. 30 worms per genotype were picked into 3 wells each at either day 1 or day 5 of adulthood. Worm motility was quantified using a PhylumTech WMicrotracker-One over a period of 10 hours.

Gene expression assays

Synchronized, age-matched animals were collected in M9 buffer at day 1 of adulthood. Animals were washed with M9 buffer 4 times to remove excess bacteria and the supernatant was removed after the last wash step. Worms were then frozen at -80°C in 500 µL TRIzol Reagent (Thermo Fisher Scientific). After thawing, worms were homogenized using a 27 ½ G needle with syringe and another 500 µL of TRIzol was added. Samples were let incubate at room temperature for 5 minutes before adding 200 µL of chloroform and letting them sit for an additional 2 minutes. Samples were then centrifuged at 12,000 g for 15 minutes allowing the phases to separate. The aqueous phase was collected, and extraction was completed using the RNeasy Mini Kit (Qiagen) and its standard protocol. cDNA was synthesized using the SuperScript VILO cDNA Synthesis Kit (Invitrogen), and gene expression to quantify *smn-1* transcript levels was done using TaqMan probes and standard TaqMan reagents (probes and reagents were purchased from Applied Biosystems). *cdc-42.1* was chosen as the housekeeping gene. Gene expression assays were run on a QuantStudio 7 Flex (Applied Biosystems) instrument and data analysis was done using QuantStudio Real-Time PCR software.

Microscopy experiments

All assays were carried out a Zeiss Axio Obeserver inverted microscope. For neurodegeneration assays, worms were immobilized in 5mM levamisole and mounted on slides with 2% agarose pads. Scoring of axonal breaks in either GABAergic or cholinergic motor neurons was done *in vivo* in day 9 animals. For neurodegeneration assays with drugs, worms were grown on NGM plates until the L4 stage and transferred to NGM + drug or NGM + DMSO control plates and maintained up to day 9 for imaging. A total of 100 animals were scored per genotype or treatment condition. For muscle degeneration assays, worms were immobilized with 0.05% sodium azide and imaged at day 3 or 5 of adulthood. Animals were scored as having either low, medium, or high levels of morphological defects. In total, 100 animals were scored. For scoring mitochondrial morphology, age-synchronized day 1 and day 5 adults were immobilized in 5 mM levamisole dissolved in M9 and mounted on slides with 2% agarose pads. The mitochondria were scored as linear, intermediate, or fragmented. A total of 100 worms were scored per condition.

Acknowledgements

We thank the *Caenorhabditis* Genetics Center at the University of Minnesota for providing strains, which is funded by NIH Office of Research Infrastructure Programs (P40 OD010440). J.J.D. is supported by a Training Award from the Fonds de recherche du Québec-Santé (FRQS). J.A.P is supported by an FRQS Senior researcher award. This work was supported by the Canadian Institutes of Health Research.

References

1. T. W. Prior, Carrier screening for spinal muscular atrophy. *Genet Med* **10**, 840-842 (2008).
2. E. A. Sugarman *et al.*, Pan-ethnic carrier screening and prenatal diagnosis for spinal muscular atrophy: clinical laboratory analysis of >72,400 specimens. *Eur J Hum Genet* **20**, 27-32 (2012).
3. R. R. Moultrie, J. Kish-Doto, H. Peay, M. A. Lewis, A Review on Spinal Muscular Atrophy: Awareness, Knowledge, and Attitudes. *J Genet Couns* **25**, 892-900 (2016).
4. S. Jablonka, M. Sendtner, Developmental regulation of SMN expression: pathophysiological implications and perspectives for therapy development in spinal muscular atrophy. *Gene Ther* **24**, 506-513 (2017).
5. S. Lefebvre *et al.*, Identification and Characterization of a Spinal Muscular Atrophy-Determining Gene. *Cell* **80**, 155-165 (1995).
6. M. A. Farrar, M. C. Kiernan, The Genetics of Spinal Muscular Atrophy: Progress and Challenges. *Neurotherapeutics* **12**, 290-302 (2015).
7. K. Peeters, T. Chamova, A. Jordanova, Clinical and genetic diversity of SMN1-negative proximal spinal muscular atrophies. *Brain* **137**, 2879-2896 (2014).
8. N. Owen, C. L. Doe, J. Mellor, K. E. Davies, Characterization of the Schizosaccharomyces pombe orthologue of the human survival motor neuron (SMN) protein. *Human Molecular Genetics* **9**, 675-684 (2000).
9. R. J. Duronio, P. H. O'Farrell, G. Sluder, T. T. Su, Sophisticated lessons from simple organisms: appreciating the value of curiosity-driven research. *Dis Model Mech* **10**, 1381-1389 (2017).
10. M. Dimitriadi *et al.*, Decreased function of survival motor neuron protein impairs endocytic pathways. *Proc Natl Acad Sci U S A* **113**, E4377–E4386 (2016).
11. M. Briese *et al.*, Deletion of smn-1, the Caenorhabditis elegans ortholog of the spinal muscular atrophy gene, results in locomotor dysfunction and reduced lifespan. *Hum Mol Genet* **18**, 97-104 (2009).
12. M. Dimitriadi *et al.*, Conserved genes act as modifiers of invertebrate SMN loss of function defects. *PLoS Genet* **6**, e1001172 (2010).
13. M. Dimitriadi *et al.*, The neuroprotective drug riluzole acts via small conductance Ca2+-activated K+ channels to ameliorate defects in spinal muscular atrophy models. *J Neurosci* **33**, 6557-6562 (2013).
14. X. Gao *et al.*, The survival motor neuron gene smn-1 interacts with the U2AF large subunit gene uaf-1 to regulate Caenorhabditis elegans lifespan and motor functions. *RNA Biol* **11**, 1148-1160 (2014).
15. P. J. O'Hern *et al.*, Decreased microRNA levels lead to deleterious increases in neuronal M2 muscarinic receptors in Spinal Muscular Atrophy models. *Elife* **6** (2017).
16. M. Riessland *et al.*, Neurocalcin Delta Suppression Protects against Spinal Muscular Atrophy in Humans and across Species by Restoring Impaired Endocytosis. *Am J Hum Genet* **100**, 297-315 (2017).

17. S.-Y. Ng *et al.*, Genome-wide RNA-Seq of Human Motor Neurons Implicates Selective ER Stress Activation in Spinal Muscular Atrophy. *Cell Stem Cell* **17**, 569-584 (2015).
18. L. A. Nash, J. K. Burns, J. W. Chardon, R. Kothary, R. J. Parks, Spinal Muscular Atrophy: More than a Disease of Motor Neurons? *Current Molecular Medicine* **16**, 779 - 792 (2016).
19. O. Thompson *et al.*, The Million Mutation Project: A New Approach to Genetics in Caenorhabditis elegans. . *Genome Research* **10**, 1749-1762 (2013).
20. A. Vaccaro *et al.*, Mutant TDP-43 and FUS cause age-dependent paralysis and neurodegeneration in C. elegans. *PLoS One* **7**, e31321 (2012).
21. B. Barbagallo, H. A. Prescott, P. Boyle, J. Climer, M. M. Francis, A dominant mutation in a neuronal acetylcholine receptor subunit leads to motor neuron degeneration in Caenorhabditis elegans. *J Neurosci* **30**, 13932-13942 (2010).
22. M. Bowerman *et al.*, Pathogenic commonalities between spinal muscular atrophy and amyotrophic lateral sclerosis: Converging roads to therapeutic development. *Eur J Med Genet* 10.1016/j.ejmg.2017.12.001 (2017).
23. T. R. Mahoney, S. Luo, M. L. Nonet, Analysis of synaptic transmission in Caenorhabditis elegans using an aldicarb-sensitivity assay. *Nat Protoc* **1**, 1772-1777 (2006).
24. A. Paix *et al.*, Scalable and versatile genome editing using linear DNAs with microhomology to Cas9 Sites in Caenorhabditis elegans. *Genetics* **198**, 1347-1356 (2014).
25. A. Paix, A. Folkmann, D. Rasoloson, G. Seydoux, High Efficiency, Homology-Directed Genome Editing in Caenorhabditis elegans Using CRISPR-Cas9 Ribonucleoprotein Complexes. *Genetics* **201**, 47-54 (2015).
26. A. Paix, A. Folkmann, G. Seydoux, Precision genome editing using CRISPR-Cas9 and linear repair templates in C. elegans. *Methods* **121-122**, 86-93 (2017).
27. D. J. Dickinson, B. Goldstein, CRISPR-Based Methods for Caenorhabditis elegans Genome Engineering. *Genetics* **202**, 885-901 (2016).
28. K. G. MILLER *et al.*, A genetic selection for Caenorhabditis elegans synaptic transmission mutants. *Proc Natl Acad Sci U S A* **93** (1996).
29. B. Meissner *et al.*, An integrated strategy to study muscle development and myofilament structure in Caenorhabditis elegans. *PLoS Genet* **5**, e1000537 (2009).
30. D. Riddle, T. Blumenthal, B. Meyer, *Section II The Organization, Structure, and Function of Muscle*, C. elegans II. 2nd edition (1997).
31. S. Sarasija, K. R. Norman, A gamma-Secretase Independent Role for Presenilin in Calcium Homeostasis Impacts Mitochondrial Function and Morphology in Caenorhabditis elegans. *Genetics* **201**, 1453-1466 (2015).
32. S. Sarasija, K. R. Norman, Analysis of Mitochondrial Structure in the Body Wall Muscle of Caenorhabditis elegans. *Bio Protoc* **8** (2018).
33. A. Vaccaro *et al.*, Pharmacological reduction of ER stress protects against TDP-43 neuronal toxicity in vivo. *Neurobiol Dis* **55**, 64-75 (2013).
34. C. E. Richardson, S. Kinkel, D. H. Kim, Physiological IRE-1-XBP-1 and PEK-1 signaling in Caenorhabditis elegans larval development and immunity. *PLoS Genet* **7**, e1002391 (2011).

35. S. A. Patten *et al.*, Neuroleptics as therapeutic compounds stabilizing neuromuscular transmission in amyotrophic lateral sclerosis. *JCI Insight* **2** (2017).
36. E. C. Burt, P. R. Towers, D. B. Sattelle, Caenorhabditis elegans in the study of SMN-interacting proteins: a role for SMI-1, an orthologue of human Gemin2 and the identification of novel components of the SMN complex. *Invert Neurosci* **6**, 145-159 (2006).
37. I. Gallotta *et al.*, Neuron-specific knock-down of SMN1 causes neuron degeneration and death through an apoptotic mechanism. *Hum Mol Genet* **25**, 2564-2577 (2016).
38. J. N. Sleigh *et al.*, A novel Caenorhabditis elegans allele, smn-1(cb131), mimicking a mild form of spinal muscular atrophy, provides a convenient drug screening platform highlighting new and pre-approved compounds. *Hum Mol Genet* **20**, 245-260 (2011).
39. M. Boyce *et al.*, A Selective Inhibitor of eIF2a Dephosphorylation Protects Cells from ER Stress. *Science* **307**, 935-939 (2005).

Figures

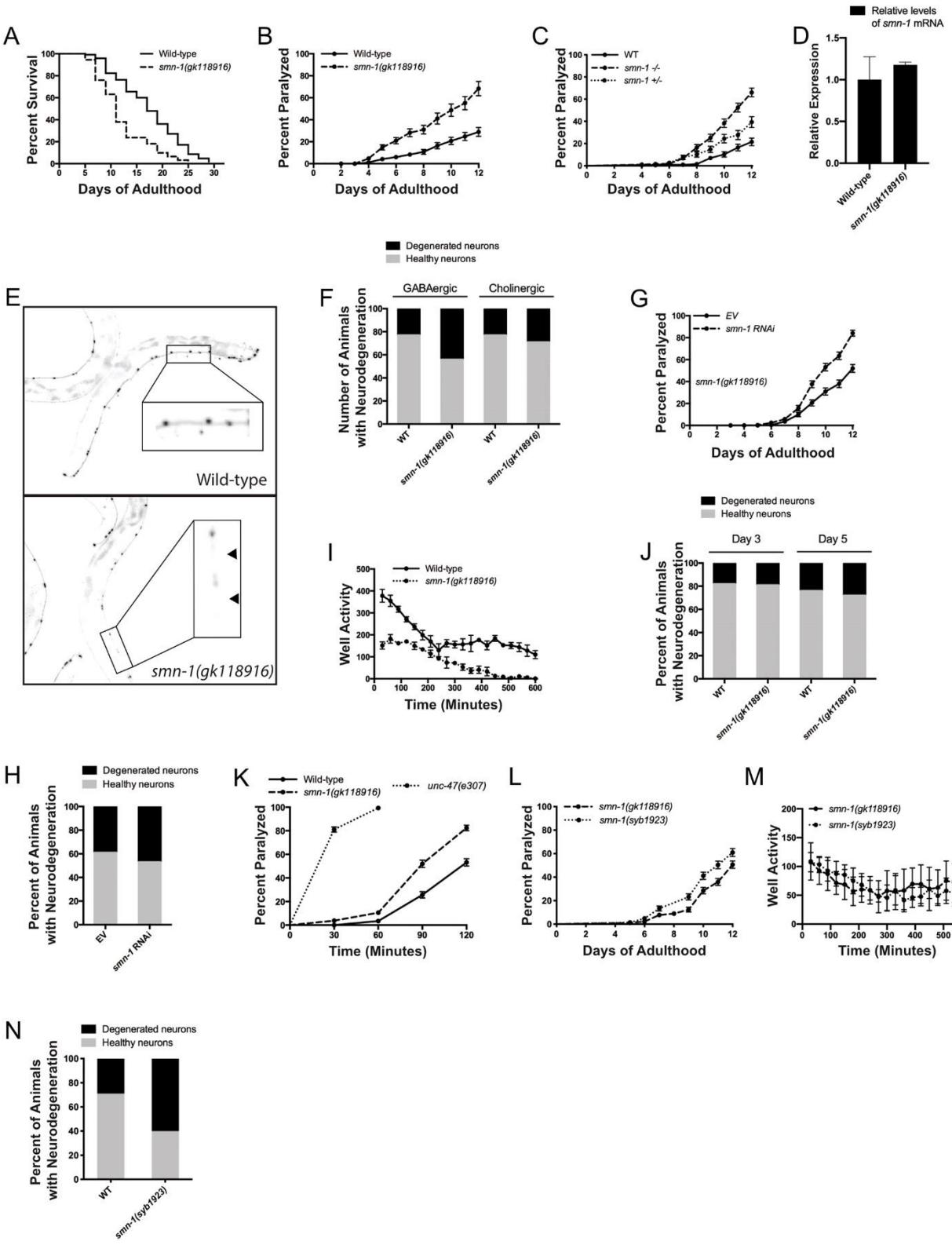

Fig. 1. A point mutation in *smn-1* recapitulates key neuronal features of SMA. (*A*) *smn-1(gk)* mutant animals display a reduction in lifespan (Mantel-Cox test, ****P<0.0001). (*B*) *smn-1(gk)* results in an increase in age-dependent paralysis compared to wild-type N2 animals (Mantel-Cox test, ****P<0.0001). (*C*) *smn-1(gk)*/+ heterozygous animals display lower paralysis levels compared to *smn-1(gk)*/ *smn-1(gk)* homozygous mutants, but higher paralysis than N2 animals (Mantel-Cox test, ****P<0.0001 and ***P<0.001, respectively). (*D*) *smn-1(gk)* mutation does not significantly affect *smn-1* mRNA expression levels (Student's *t* test, n.s.). (*E*) Representative images of GABAergic neurodegeneration observed in day 9 adult WT and *smn-1(gk)* mutant animals. Black arrows indicate neuronal gaps indicative of neurodegeneration. (*F*) *smn-1(gk)* mutant animals display GABAergic motor neuron degeneration ay day 9 (Student *t* test, ***P<0.001, n=100 animals per condition), but do not show any degeneration of cholinergic motor neurons (Student *t* test, n.s., n=100 animals per condition). (*G*) Non-neuronal RNAi treatment of *smn-1(gk)* animals with *smn-1* RNAi exacerbates paralysis (Mantel-Cox test, ****P<0.0001). (*H*) Non-neuronal *smn-1* RNAi treatment does not increase GABAergic motor neuron degeneration in *smn-1(gk)* mutant (Students *t* test, n.s., n=100 animals per condition). (*I*) Swimming defects in *smn-1(gk)* animals are observed at day 5 of adulthood (Two-way ANOVA, ****P<0.0001). (*J*) *smn-1(gk)* mutant animals do not display degeneration of GABAergic motor neurons at days 3 or 5 (Students *t* test, n.s., n=100 animals per condition). (*K*) At day 1 of adulthood, *smn-1(gk)* mutants display hypersensitivity to aldicarb compared to N2 animals, but not to the same extent as *unc-47(e307)* animals (Mantel-Cox test, ****P<0.0001, and ****P<0.0001, respectively). (*L*) *smn-1(syb1923)* animals show slightly higher levels of paralysis than *smn-1(gk)* animals (Mantel-Cox test, **P<0.01). (*M*) Swimming defects in *smn-1(syb1923)*

are nearly identical as those in *smn-1(gk)* mutants (Two-way ANOVA, n.s.). (*N*) *smn-1(syb1923)* animals display GABAergic neuron degeneration (Two-way ANOVA, $^{**}P<0.01$, n=100 animals per condition).

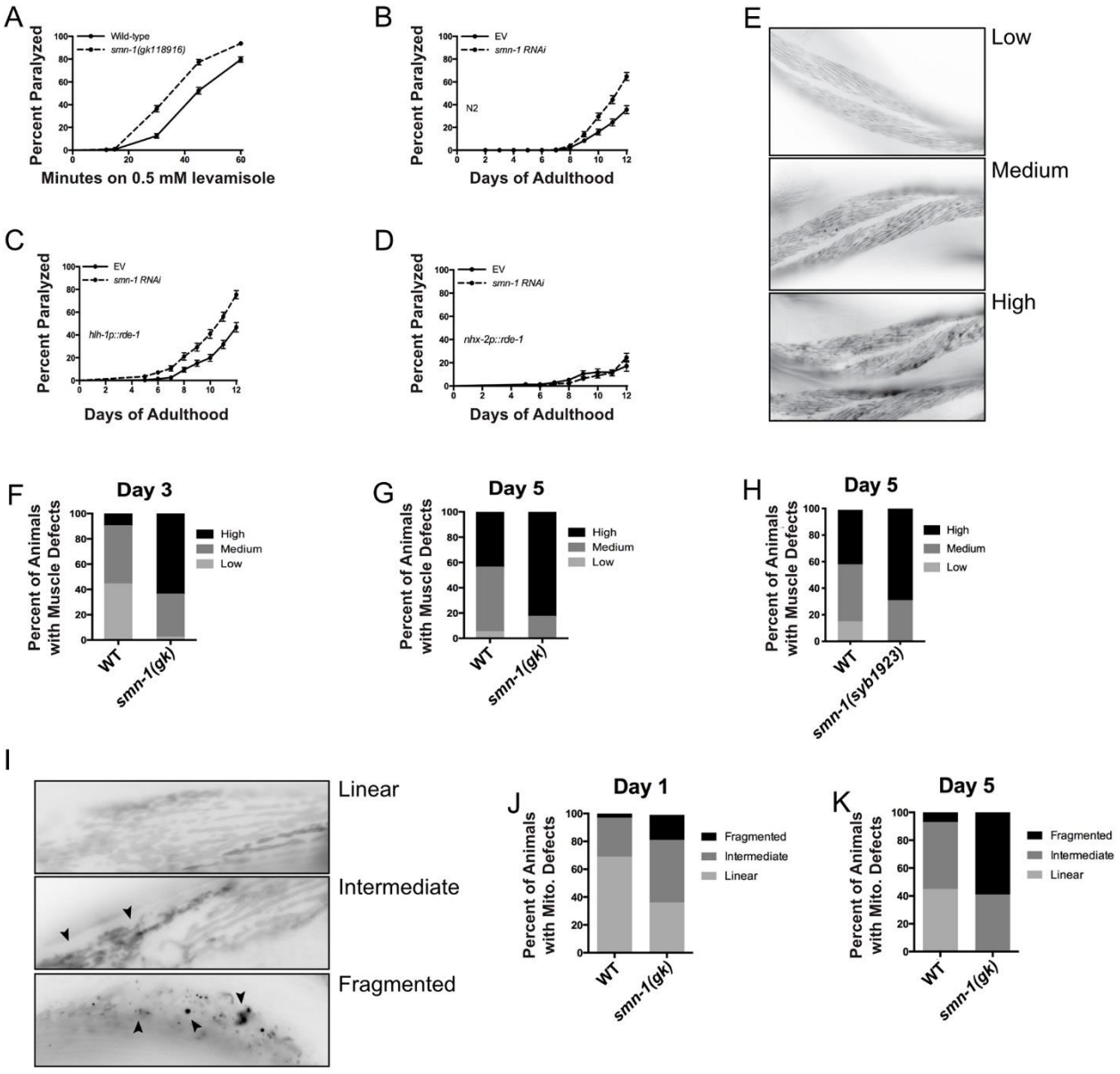

Fig. 2. *smn-1(gk)* mutants show signs of early muscle defects. (A) Day 1 adult *smn-1(gk)* mutant animals are hypersensitive to the nAChR agonist levamisole (Mantel-Cox test, ****P<0.0001). (B) WT N2 animals paralyze when they are fed RNAi against *smn-1* (Mantel-Cox test, ****P<0.0001). (C) Transgenic worms sensitive to RNAi only in their body-wall muscle cells paralyzed when they were fed RNAi against *smn-1* (Mantel-Cox test, ****P<0.0001). (D) RNAi KD of *smn-1* in intestinal

cells does not result in a paralysis phenotype (Mantel-Cox text, n.s.). (E) Representative images of transgenic animals expressing GFP::MYO-3 in their body-wall muscle cells. Levels of morphological distortion were characterized as "Low", "Medium", or "High" depending on the extent of GFP::MYO-3 disorganization in the cells. (F-G) At both days 3 and 5 of adulthood, *smn-1(gk)* mutant animals displayed greater levels of animals with "High" levels of muscle dysfunction (Two-way ANOVA, ****P<0.0001 and ****P<0.0001, respectively; n=100 animals per condition). (H) smn-1(syb1923) CRISPR mutants display increased muscle dysfunction compared to WT animals (Two-way ANOVA, ****P<0.0001). (I) Representative images of transgenic animals expressing TOM20::mRFP in body-wall muscle cells. Mitochondrial organization was quantified as either "Linear", "Intermediate", or "Fragmented". (J-K) At both days 1 and 5, *smn-1(gk)* mutants had higher levels of mitochondria impairment compared to WT animals (Two-way ANOVA ****P<0.0001 and ****P<0.0001, respectively; n=100 animals per condition).

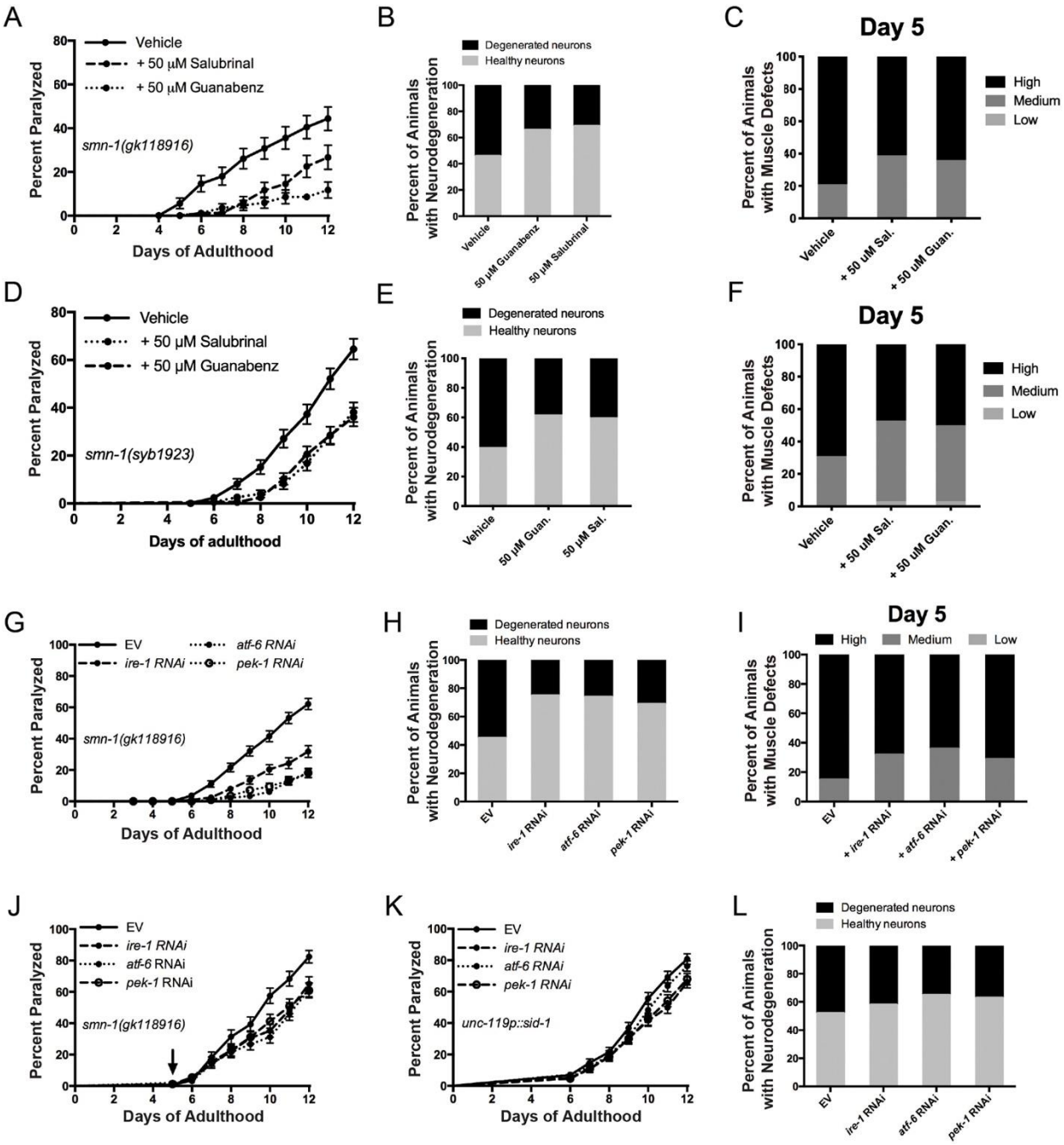

Fig. 3. Targeting ER stress chemically and genetically is protective in *smn-1* mutants, and is more effective when targeted to non-neuronal cells. (*A*) Treatment of *smn-1(gk)* mutant animals with either 50 µM guanabenz or salubrinal attenuates the paralysis phenotype (Mantel-Cox test, ****P<0.0001 and **P<0.01, respectively). (*B*) Pharmacological inhibition of ER stress with either

50 µM guanabenz or salubrinal prevents neurodegeneration in GABAergic motor neurons in *smn-1(gk)* mutants (Student *t* test, **P*<0.05 and ***P*<0.01, respectively; n=100 animals per condition). (C) Salubrinal and guanabenz treatment partially restores muscle morphology in *smn-1(gk)* mutants (Two-way ANOVA, *****P*<0.0001 and *****P*<0.0001, respectively). (D) Treating *smn-1(syb1923)* animals with either 50 µM guanabenz or salubrinal ameliorates their paralysis phenotype (Mantel-Cox test, *****P*<0.0001 and *****P*<0.0001). (E) Salubrinal and guanabenz treatments restore neurodegeneration at day 9 in *smn-1(syb1923)* animals (Student *t* test, ****P*<0.001 and *****P*<0.0001, respectively; n=100 animals per condition). (F) Salubrinal and guanabenz treatments partially restores muscle dysfunction of *smn-1(syb1923)* mutants (Two-way ANOVA, ***P*<0.01 and **P*<0.05). (*G*) Non-neuronal RNAi against *ire-1*, *atf-6*, and *pek-1* restores paralysis in *smn-1(gk)* animals compared to EV treatment (Mantel-Cox test, *****P*<0.0001). (H) Treatment of *smn-1(gk)* animals with non-neuronal *ire-1*, *atf-6*, and *pek-1* RNAi also protects against neurodegeneration (Student *t* test, *****P*<0.0001, ****P*<0.001, and ***P*<0.01. respectively; n=100 animals per condition). (I) Treating *smn-1(gk)* mutants with non-neuronal *ire-1*, *atf-6*, and *pek-1* RNAi helps restore muscle defects (Two-way ANOVA, *****P*<0.0001, *****P*<0.0001, and *****P*<0.0001, respectively; n=100 animals per condition). (J) Non-neuronal *ire-1*, *atf-6*, and *pek-1* RNAi treatment as of day 5 of adulthood is still capable of partially attenuating paralysis phenotypes in *smn-1(gk)* mutants (Mantel-Cox test, ***P*<0.01, ****P*<0.001, and ***P*<0.01, respectively). (K) Neuronal *ire-1*, *atf-6*, and *pek-* RNAi treatment had no effect on *smn-1(gk)* paralysis compared to EV treatment (Mantel-Cox test, n.s. for all treatments). (L) Neuronal KD of *ire-1*, *atf-6*, *pek-1* in *smn-1(gk)* animals does not significantly rescue neurodegeneration (Students *t* test, n.s.; n=100 animals per condition).

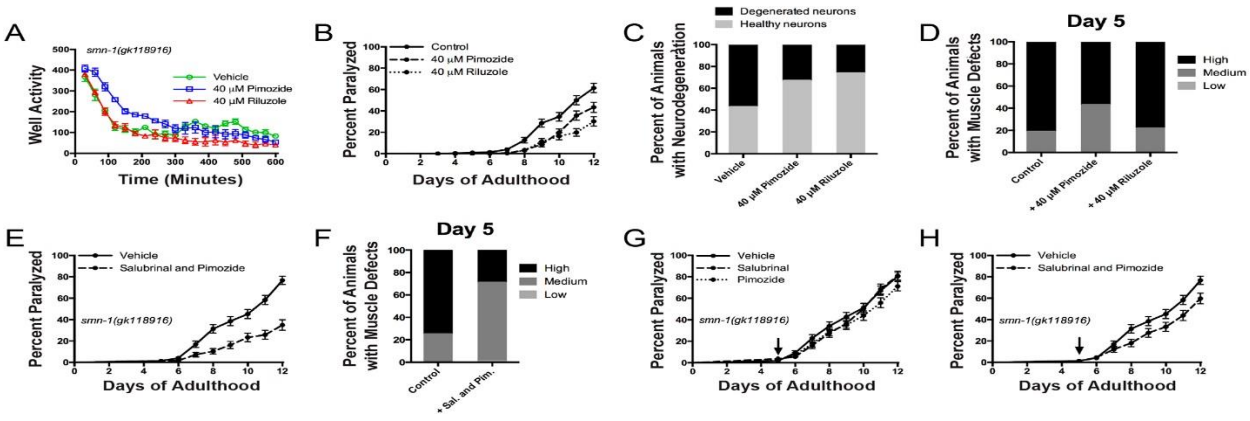

Fig. 4. Simultaneously targeting ER stress and NMJ stabilization have an additive effect on *smn-smn-1(gk)* mutants. (*A*) Treatment of *smn-1(gk)* mutant animals with 40 µM pimozide significantly improved the animals' swimming behavior (Two-way ANOVA, ****P<0.0001), whereas 40 µM riluzole treatment significantly reduced it (Two-way ANOVA, ****P<0.0001). (*B*) Treatment with 40 µM pimozide or riluzole was able to significantly reduce paralysis in *smn-1(gk)* animals (Mantel-Cox test, ***P<0.001 and ****P<0.0001, respectively). (*C*) GABAergic motor neuron degeneration was significantly reduced in *smn-1(gk)* mutant animals upon pimozide or riluzole treatment (Student *t* test, **P<0.01 and ***P<0.001, respectively). (*D*) Muscle dysfunction was partially restored in *smn-1(gk)* animals upon treatment with pimozide, but riluzole had no effect (Two-way ANOVA, ****P<0.0001 and n.s., respectively). (*E*) Treatment of *smn-1(gk)* animals simultaneously with both 20 µM pimozide and 25 µM salubrinal restored effectively restored paralysis (Mantel-Cox test, ****P<0.0001). (*F*) Simultaneous treatment with both salubrinal and pimozide greatly restores muscle defects in *smn-1(gk)* mutants (Two-way ANOVA, ****P<0.0001). (G) Individually, treatment of *smn-1(gk)* mutants with salubrinal and pimozide as of day 5 had no effect on paralysis (Mantel-Cox test, n.s.). (H) Treatment of *smn-1(gk)* with both pimozide and salubrinal as of day 5 resulted in a slight decrease of paralysis levels (Mantel-Cox test, **P<0.01).